Attrition Resistance of Supports for Iron Fischer–Tropsch Catalysts

ARTICLE *in* INDUSTRIAL & ENGINEERING CHEMISTRY RESEARCH · JULY 2003

Impact Factor: 2.59 · DOI: 10.1021/ie020875h

Attrition Resistance of Supports for Iron Fischer−Tropsch Catalysts

Hien N. Pham,[†] Lech Nowicki,[‡] Jian Xu,[§] Abhaya K. Datye,*[,†] Dragomir B. Bukur,[‡] and Calvin Bartholomew[§]

Center for Microengineered Materials and Department of Chemical & Nuclear Engineering, University of New Mexico, Albuquerque, New Mexico 87131, Department of Chemical Engineering, Texas A&M University, College Station, Texas 77843, and Department of Chemical Engineering, Brigham Young University, Provo, Utah 84602

Seven commercially available aluminas and silicas were screened for their potential use as supports for preparing attrition-resistant iron Fischer−Tropsch (F−T) catalysts. First we used ultrasonic irradiation to determine the attrition resistance of these supports. Among the supports tested, one alumina support and two silica supports were found to possess adequate attrition resistance. These supports were then tested in a stirred tank slurry reactor (STSR) under nonreactive conditions, using N_2 gas at 260 °C, 1.5 MPa, and 3 L(STP)/(g of catalyst)·h. Particle size distributions of these supports provided a measure of attrition during simulated F−T synthesis runs. Particle size distributions allow us to infer the extent of fracture and erosion during attrition tests. Our work showed that the ultrasonic irradiation test was less severe than the STSR test in terms of generation of small (1−10 μm) particles (erosion).

Introduction

The Fischer−Tropsch (F−T) synthesis reaction is attracting increasing attention as a possible route for conversion of natural gas and coal into liquid fuels. Iron (Fe) is an active catalyst for this reaction; however, attrition of Fe F−T catalysts has been identified as a major problem in commercial implementation of slurry bubble-column reactors (SBCRs).[1−3] It is also recognized that precipitated Fe catalysts, while possessing high activity for F−T synthesis, may not possess the optimal morphology for use in SBCRs. Our work is directed at supported Fe catalysts, and as a first step, we have studied commercially available silica and alumina materials for their suitability for preparing attrition-resistant Fe F−T catalysts. The attrition resistance of these supports was studied via ultrasonic fragmentation,[4,5] a method we have shown to be useful for rapid screening of attrition behavior.[6] The more promising supports from these initial screening studies were then tested in a stirred tank slurry reactor (STSR), where nitrogen gas was bubbled to simulate the mechanical forces that would be encountered during slurry reactor operation. In subsequent work, catalyst supports of adequate attrition resistance will be used to prepare supported Fe F−T catalysts.

Previous Work

In a previous study, Pham et al.[6,7] reported on the synthesis of attrition-resistant Fe catalysts for F−T synthesis, a reaction that allows conversion of coal or natural gas into liquid fuels. These catalysts were prepared by spray drying, and the processing steps were examined to correlate the microstructure with the attrition resistance of the catalysts.[8] Other researchers have also used spray drying to prepare Fe F−T catalysts.[9,10] Recently, Zhao et al.[11] investigated in greater detail the catalyst properties affecting the attrition resistance of spray-dried Fe catalysts. They found that particle density, among all of the particle properties, was the most significant in determining the catalyst attrition resistance. A higher particle density resulted in a more compact catalyst structure that provided better mechanical strength. In addition, they found that the silica type and concentration were critical in the improvement of the attrition resistance of the spray-dried Fe catalysts.

It is important to improve the attrition resistance of the Fe F−T catalysts without sacrificing either the activity or the selectivity of these catalysts. Recently, O'Brien et al.[12] characterized the activity, selectivity, and attrition of several supported Fe catalysts in a STSR. They found that a precipitated Fe catalyst was more active and produced less methane than the supported catalysts. Bukur and Sivaraj[13] reported that the initial activity of a silica (Davison 952)-supported catalyst (per gram Fe basis) was higher than that of the two most active precipitated Fe catalysts synthesized at Texas A&M University. However, the silica-supported catalyst had higher methane and gaseous hydrocarbon selectivity than the precipitated Fe catalysts. Alumina-supported catalysts[12,13] had better selectivities than the silica-supported catalysts, but their activities were lower.

O'Brien et al.[12] reported the range of particle sizes for the alumina and magnesium aluminate containing catalysts before and after reaction tests, which were presumably derived from scanning electron microscope (SEM) images. The SEM images of the silica and magnesium silicate containing catalysts before and after the STSR runs suggest that there was little attrition during reaction STSR tests. However, it is difficult to derive accurate particle size distributions from SEM images because weakly agglomerated particles will not clearly show up in these images.

* To whom correspondence should be addressed at Center for Microengineered Materials. Tel.: (505) 277-0477. Fax (505) 277-1024. E-mail: datye@unm.edu.
[†] University of New Mexico.
[‡] Texas A&M University.
[§] Brigham Young University.

10.1021/ie020875h CCC: $25.00
Published on Web 07/29/2003

Table 1. Properties of Alumina Supports[a]

	Condea Vista HP 14		Condea Vista B	Condea Vista HP 14-150	
	uncalcd	calcd[b]	uncalcd	uncalcd	calcd[b]
density (g/cm^3)	2.71	2.68		3.07	3.07
type	Boehmite	Boehmite	Boehmite	γ-alumina	γ-alumina
pore volume (cm^3/g)	0.94		0.47	0.97	
surface area (m^2/g)	150	156	243	153	157

[a] Vista HP 14 and HP 14-150 are microspherical particles (via spray drying). [b] 500 °C for 5 h.

Table 2. Properties of Silica Supports

	Grace Davison 644	Grace Davison 654	Grace Davison 948		Grace Davison 952
	uncalcd	uncalcd	uncalcd	calcd[a]	uncalcd
type	silica gel	silica gel	silica gel	silica gel	silica gel
density (g/cm^3)	2.29	2.23	2.09	2.08	2.32
pore volume (cm^3/g)	1.10	1.70	1.62		1.61
surface area (m^2/g)	268	272	279	304	309

[a] 500 °C for 5 h.

To provide insight into the relative extent of fracture and erosion, we have used a Sedigraph 5100 particle size analyzer, which directly measures the particle size distribution. We first used ultrasonic fragmentation because it can evaluate, in a very short time, the attrition behavior of these catalysts. However, there is some concern about the suitability of the ultrasonic fragmentation approach for predicting the attrition properties of particles in a slurry reactor. We therefore present a comparison of the ultrasonic tests with the attrition behavior of supports subjected to long-term tests in a STSR. By following particle size distributions as a function of time on stream in a slurry reactor, we gain insight into the extent of attrition during STSR runs. In this work, we present an evaluation of several commercially available silica and alumina supports for their suitability in preparing attrition-resistant Fe F−T catalysts.

Experimental Section

Four silica supports and three alumina supports were used for the attrition tests: Grace Davison 644, 654, 948, and 952 silicas and Condea (now Sasolchemie Gmbh) Vista B, HP 14, and HP 14-150 aluminas. Tables 1 and 2 show the physical properties of the alumina and silica supports, respectively. For the ultrasonic fragmentation tests, 1 g of support was added to 50 mL of a 0.05 wt % sodium hexametaphosphate solution, which was used as a dispersant. A Micromeritics Sedigraph 5100 analyzer was used to measure the initial (at time 0 min) particle size distribution. The suspension was then subjected to ultrasonic energy at an amplitude setting of 20 (100 W) at 5 min intervals using a Tekmar 501 ultrasonic disrupter (20 kHz ± 50 Hz) equipped with a V1A horn and a $^1/_2$-in. probe tip. After different extents of ultrasonic irradiation, the particle size distribution was analyzed to detect the mode of particle fragmentation.

After screening of attrition properties of supports by an ultrasound irradiation method, the most promising supports were tested in a STSR. Experiments were conducted in a 1-dm^3 reactor (Autoclave Engineers, Erie, PA). The experimental setup for the STSR tests has been described in detail elsewhere.[14−16] A standard six-blade turbine impeller of 3.2-cm diameter and a stirrer speed of 1200 rpm were used in all experiments. In a typical experiment, the reactor was charged with 25 g of support dispersed in 450−470 g of Durasyn-164 (hydrogenated 1-decene homopolymer). Nitrogen at 260 °C, 1.5 MPa, and 3 NL/g/h was used as the feed gas in experiments under nonreactive conditions (NL = normal liter at standard temperature, 0 °C, and pressure, 1

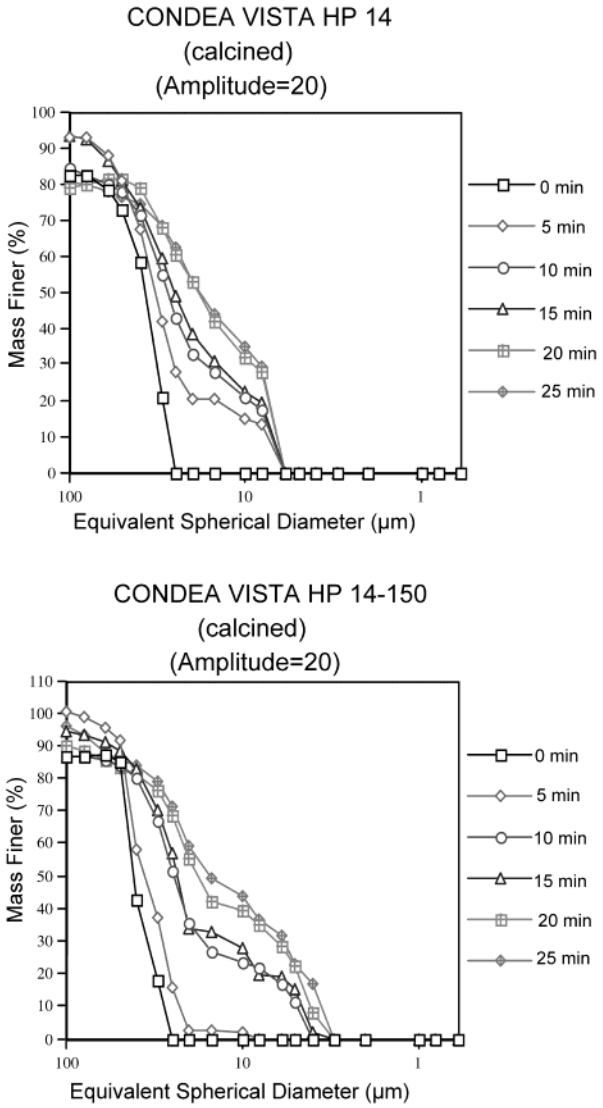

Figure 1. Sedigraph particle size distributions of Vista HP 14 and HP 14-150 alumina supports. The shift in the median particle size to smaller particles indicates fracture of the primary agglomerates, which occurs more readily with Vista HP 14-150 than with Vista HP 14.

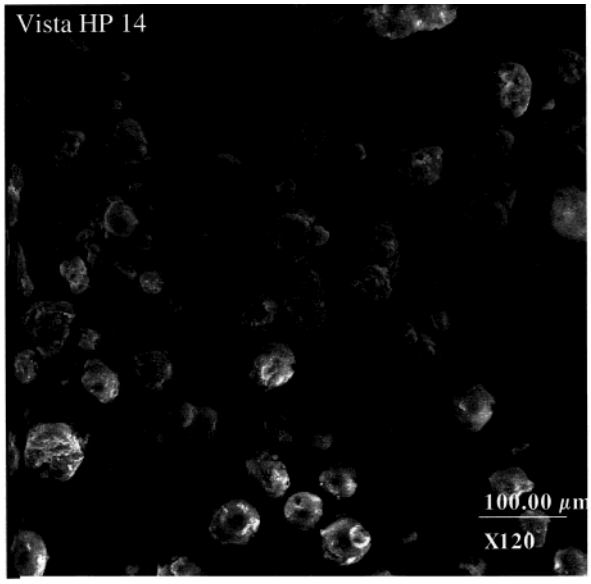

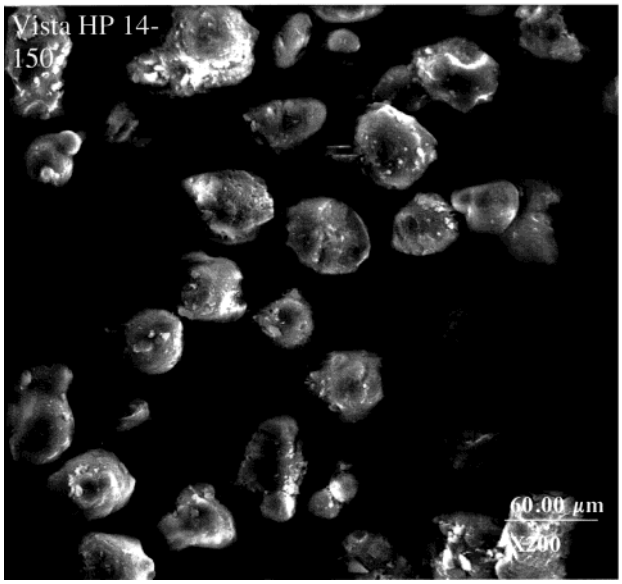

Figure 2. SEM images of Vista HP 14 and HP 14-150 alumina supports, as-received. Both aluminas are roughly spherical in shape.

bar). Slurry samples were withdrawn from the STSR at 0, 8, 24, and 168 h of stirring, and Durasyn-164 was removed by filtration aided by the addition of a commercial solvent Varsol (mixture of liquid hydrocarbons and oxygenates).

Density measurements, for calculating particle size distributions via sedimentation analysis, were performed using a Micromeritics AccuPyc 1330 pycnometer with a 1-cm^3 sample cup. The pycnometer was initially calibrated using a precision steel sphere of known volume. The cup was then filled with a sample such that the cup was at least two-thirds full. Both weighing and loading of the sample into the cell chamber of the pycnometer were done as quickly as possible to avoid exposure to atmospheric moisture. The density was then determined using helium, with five consecutive runs during the analysis to obtain a more accurate result.

Results

Ultrasonic Fragmentation Runs. Figure 1 shows cumulative mass distribution plots of Vista HP 14 and

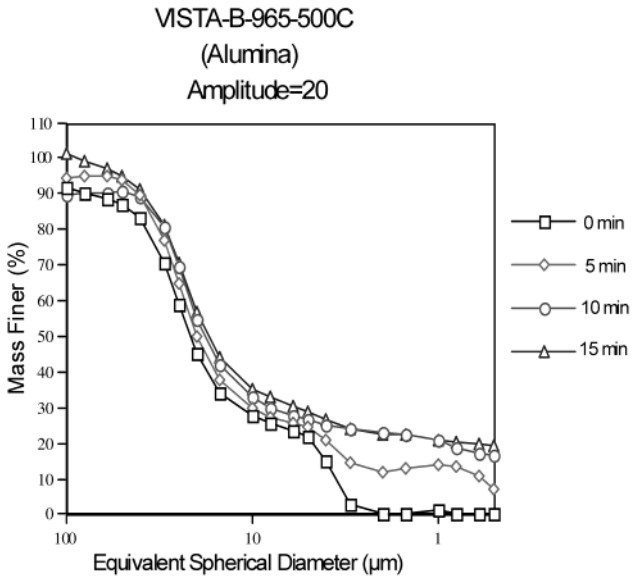

Figure 3. Sedigraph particle size distribution for Vista B alumina as a function of ultrasonic irradiation time. The starting alumina from Vista was sieved and calcined in air at 500 °C before use in this test.

Vista HP 14-150 aluminas, respectively. These plots show the mass percent of the sample that is finer than a given size as a function of exposure to ultrasonic irradiation. The shift in the median particle size to smaller particles with increasing time is indicative of the fracture of larger particles into smaller fragments. Shifts to smaller fragments are more evident with Vista HP 14-150 than with Vista HP 14. However, neither alumina leads to generation of fine particles below 6 μm, indicating that very little erosion of the primary agglomerates occurs during ultrasonic irradiation. SEM images (Figure 2) of these alumina particles before exposure to ultrasonic irradiation show that they are roughly spherical in shape. Spherical particles are preferred for use in SBCRs.

Figure 3 shows a cumulative particle size distribution plot for Vista B alumina. In our previous work,[17] this alumina was used as a test sample for comparing the strength of other slurry phase heterogeneous catalysts. In this figure, we see that the extent of particle fracture is much less pronounced than that in Figure 1. However, unlike Vista HP 14 and HP 14-150, fine particles smaller than 3 μm were generated throughout the ultrasonic fragmentation process with the Vista B alumina. These results suggest that this support is not as resistant to erosion as the Vista HP 14 and HP 14-150 supports. The SEM image (Figure 4) shows that the Vista B particles are irregularly shaped, suggesting that this alumina may not be as suitable as the HP-14 for use in a slurry reactor.

Figure 5 shows cumulative particle size distribution plots of Davison 644 and 654 silicas. The median particle sizes for Davison 644 and 654 are 38 and 42 μm, respectively. For Davison 644, there is fracture of particles after 5 min of ultrasonic irradiation, but little fracture occurs thereafter. There also appears to be very little generation of fine particles below 8 μm, suggesting that Davison 644 is attrition-resistant to erosion. On the other hand, Davison 654 is not attrition-resistant to either fracture or erosion after 25 min of ultrasonic irradiation. SEM images (Figure 6) show that Davison

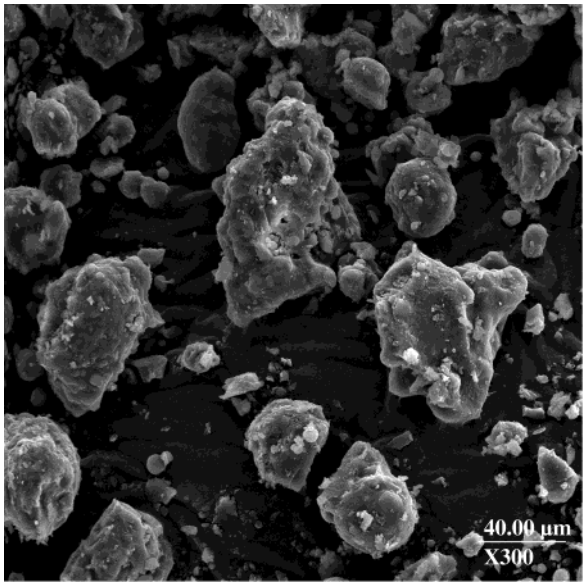

Figure 4. SEM picture of Vista B alumina, as-received. This alumina shows particles that are considerably more irregular when compared to Vista HP 14 and Vista HP 14-150.

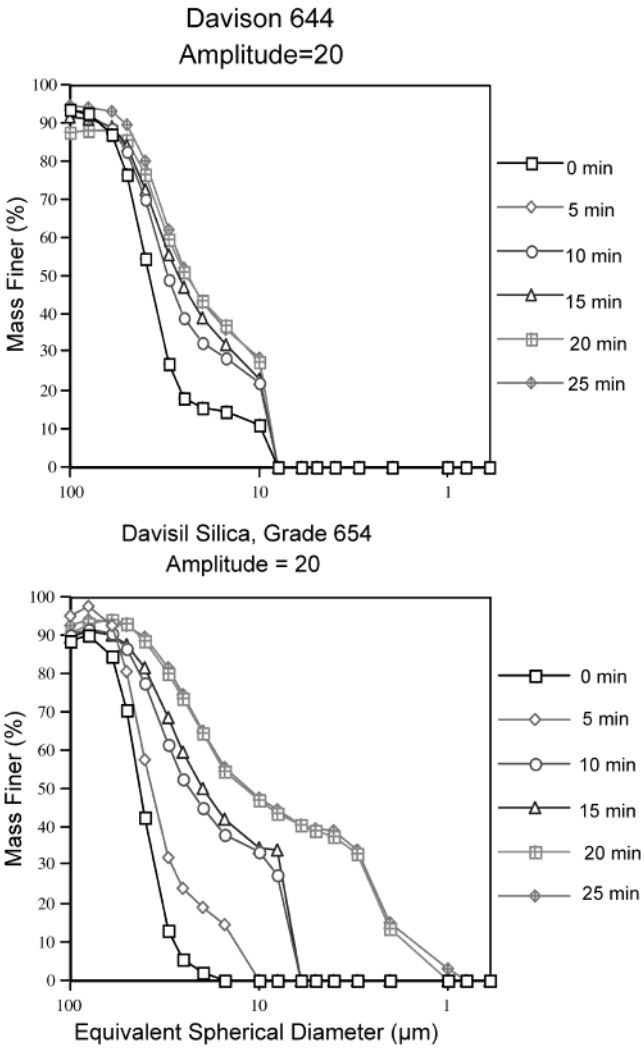

Figure 5. Sedigraph particle size distributions of Davison 644 and 654 silica supports. Davison 644 appears to be more attrition-resistant to fracture and erosion than Davison 654.

644 and 654 particles are irregularly shaped, similar to those seen for Vista B alumina by SEM.

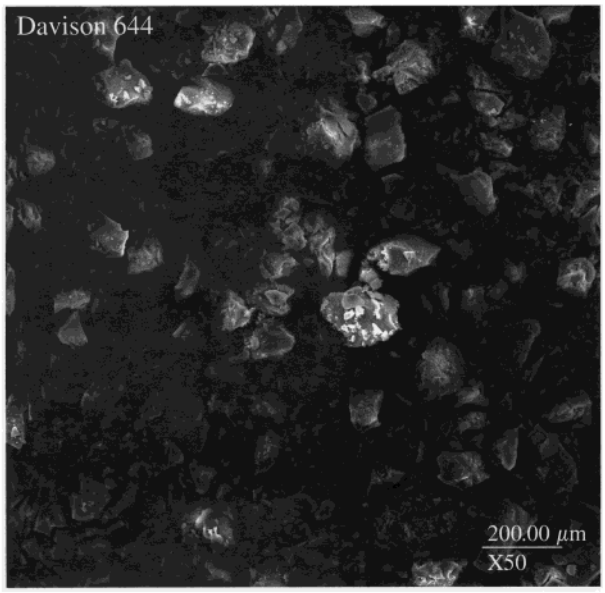

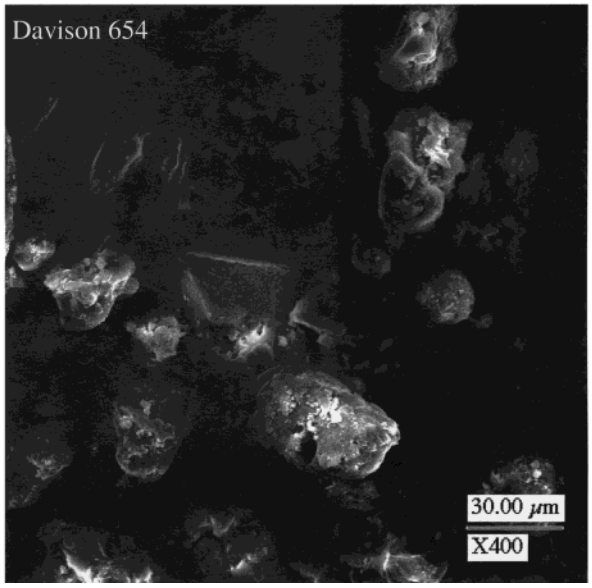

Figure 6. SEM images of Davison 644 and 654 silica supports. Both silicas are irregularly shaped, similar to those seen for Vista B alumina.

Figure 7 shows cumulative particle size distribution plots of Davison 948 and 952 silicas. For Davison 948, very little attrition of particles due to fracture is seen after 25 min of ultrasonic irradiation. Also, little generation of fine particles due to erosion is seen below 6 μm. Davison 952 is not attrition-resistant to either fracture or erosion. The median particle sizes for Davison 948 and 952 are 33 and 44 μm, respectively. SEM images (Figure 8) show that Davison 948 particles are roughly spherical, whereas Davison 952 particles are irregularly shaped.

Summary of Attrition Behavior during Ultrasonic Irradiation Tests. Of the alumina supports we have studied, Vista B alumina is more resistant to fracture than Vista HP 14 or HP 14-150. However, Vista B alumina is not resistant to erosion. Generation of particles smaller than 5 μm occurs for Vista HP 14-150, whereas no particles smaller than 5 μm are observed with Vista HP 14, both after 25 min of ultrasonic irradiation. Generation of fine particles due to erosion below 5 μm may not be acceptable for slurry F−T

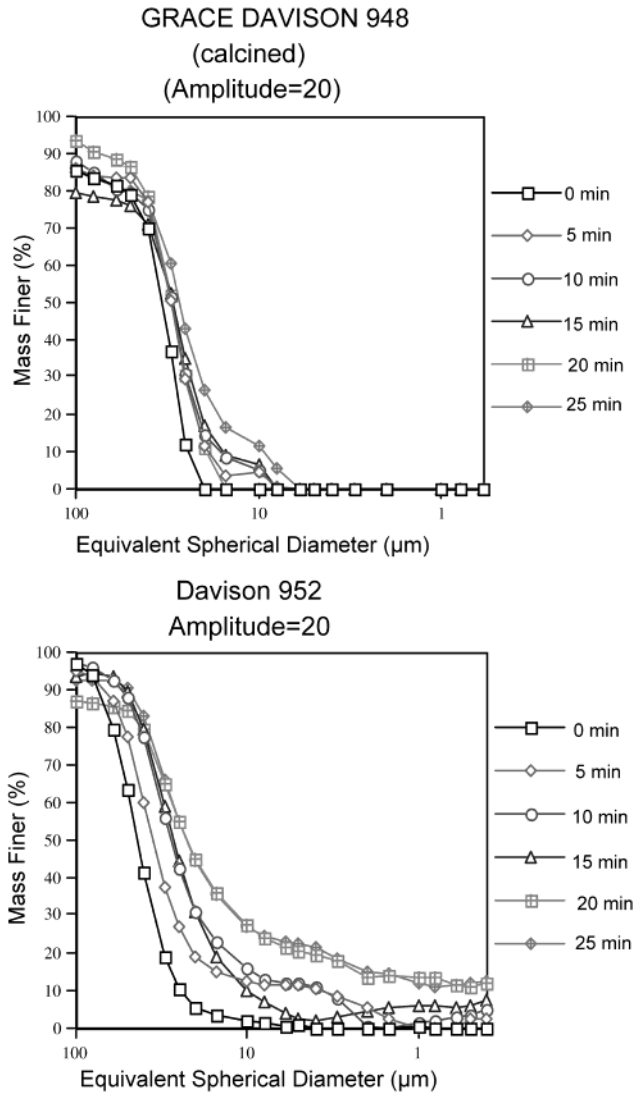

Figure 7. Sedigraph particle size distributions of Davison 948 and 952 silica supports. Davison 948 appears to be more attrition-resistant to fracture and erosion than Davison 952.

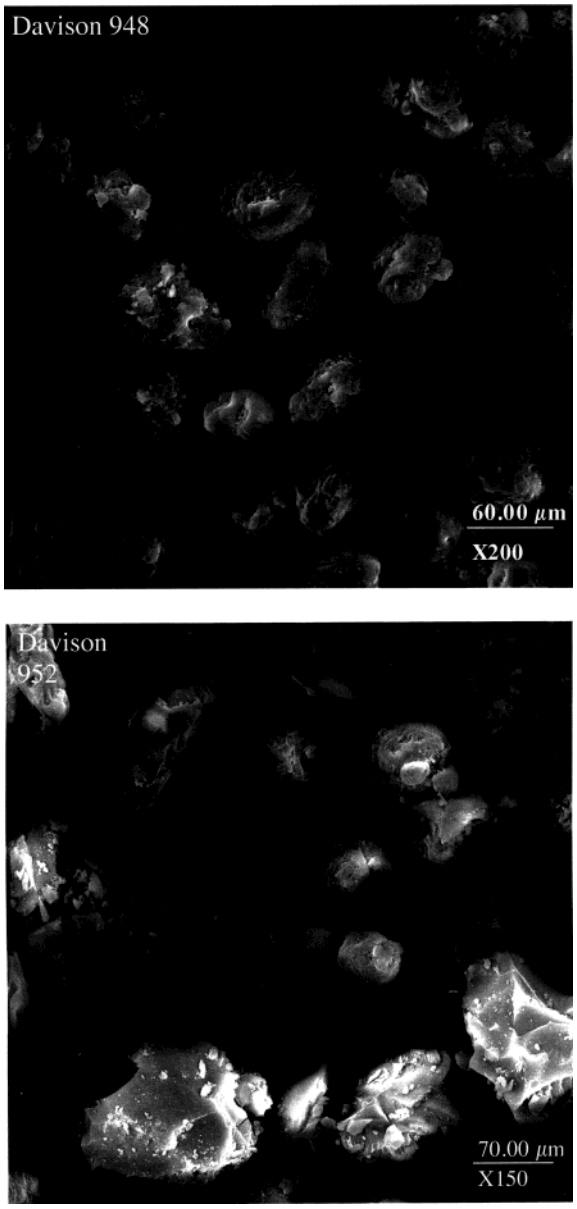

Figure 8. SEM images of Davison 948 and 952 silica supports, as-received. Davison 948 is roughly spherical in shape, while Davison 952 is irregularly shaped.

reactors based on the work reported in U.S. Patent 5,348,928. This patent discloses a process for optimally operating a three-phase slurry bubble column, where the inventors found that although smaller catalyst particles improve fluidization these particles also increase the difficulty in separation of the catalyst from the liquid product stream. Thus, particles with diameters of less than 5 μm should be avoided. Because no generation of particles below 5 μm has been observed for Vista HP 14, this type of alumina may be the most suitable as a support for preparing the attrition-resistant Fe F−T catalysts.

Of the silica supports we have studied, Davison 654 is the least attrition-resistant to fracture, while Davison 952 is the least attrition-resistant to erosion, during the ultrasonic fragmentation tests. Very little generation of fine particles below 5 μm due to erosion was observed for Davison 644 and 948 supports. Furthermore, these silicas were generally attrition-resistant to fracture throughout the ultrasonic fragmentation process. Some fracture of Davison 644 was initially observed after 5 min of ultrasonic irradiation, but not thereafter. Thus, Davison 644 and 948 may also be suitable for preparing attrition-resistant Fe catalysts.

Zhao et al.[18] did studies for predicting catalyst attrition in a three-phase SBCR using various attrition tests. In their case, they used a silica-supported cobalt catalyst. They found that the fluidized bed, jet cup, and ultrasonic attrition tests provided reasonable and efficient predictions of catalyst attrition in the SBCR. There were some differences in the attrition processes using different methods, similar to what we have observed through our methods. However, Zhao et al.[18] mainly focused on the amount of fines generated in a dry environment (flowing air), whereas our work was performed under both aqueous and nonaqueous conditions that were closer to the actual operating conditions encountered by our catalysts.

Simulated F−T Synthesis Tests. Two of the alumina and two silica supports were subjected to simulated F−T process conditions in a STSR using Durasyn-164 oil as the slurry liquid medium and N_2 as gas. Test conditions used (pressure, temperature, and gas flow rate) are representative of industrial practice with Fe F−T catalysts, except that N_2 was used instead of

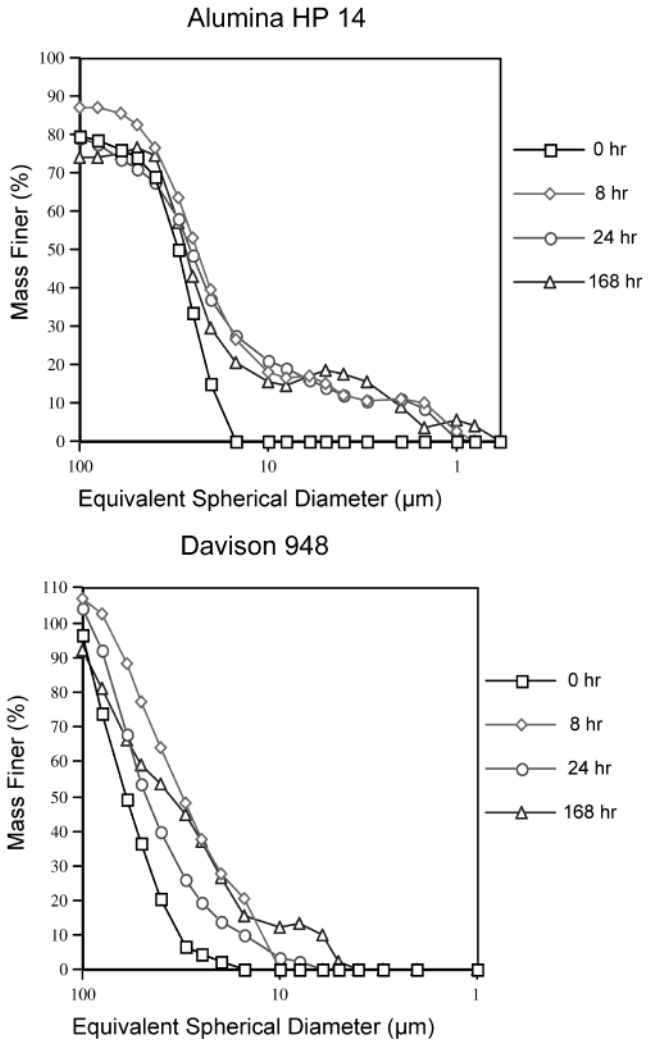

Figure 9. Sedigraph particle size distributions of Vista HP 14 and Davison 948, performed in a STSR under nonreactive F−T conditions. The production of fines is not as pronounced in the silica support. In both cases, this seems to be a result of erosion of these particles as they are subjected to agitation in the STSR.

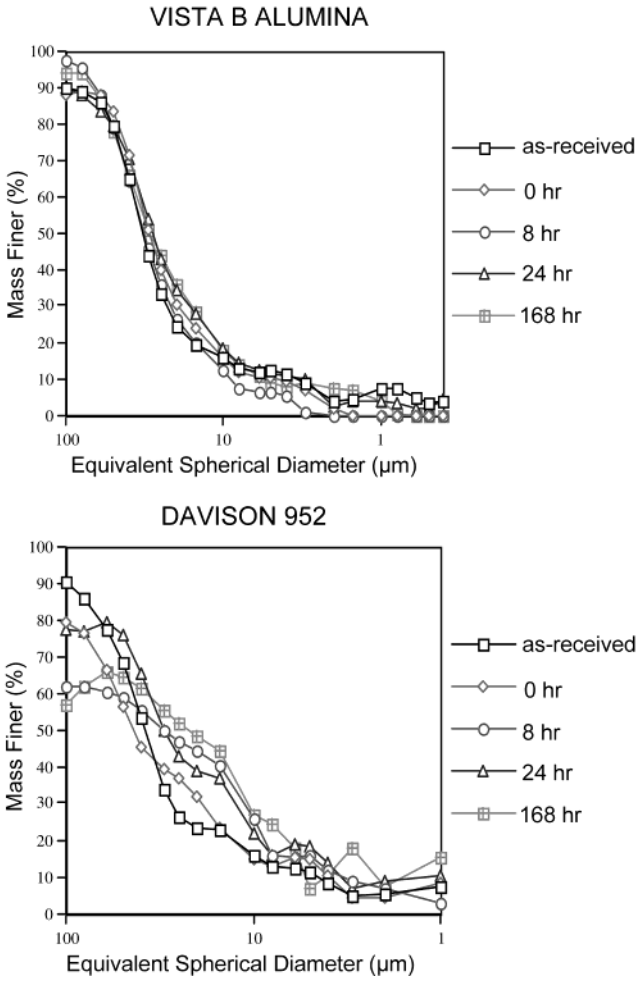

Figure 10. Sedigraph particle size distributions of Vista B alumina and Davison 952 silica, performed in a STSR under nonreacting conditions. The alumina support appears to be more attrition-resistant after the STSR runs than after the ultrasonic fragmentation runs. On the other hand, results for the silica support are similar for the STSR and ultrasonic fragmentation runs.

synthesis gas. After extraction of the supports from Durasyn-164, the particle size distributions were measured with the same Sedigraph 5100 analyzer as that used for the ultrasonic fragmentation tests, with all other experimental conditions being maintained the same.

Figure 9 shows cumulative particle size distribution plots of Vista HP 14 alumina and Davison 948 silica. In this case, Vista HP 14 shows no significant fracture, but there is generation of fine particles in the 1−10-μm range after use in the STSR for 168 h. In contrast, the generation of fine particles is less pronounced with Davison 948, but fracture is more severe. Cumulative particle size distribution plots for Vista B alumina and Davison 952 silica are shown in Figure 10. The Vista B alumina is resistant to fracture because the median particle size does not increase with time on stream, but some erosion occurs because small particles appear after stirring in oil. Davison 952 is clearly not attrition-resistant because both particle fracture and generation of fines were observed with increasing time in the STSR. This behavior confirms the trends seen in ultrasonic fragmentation tests. Note that the particle size distribution for the as-received Davison 952 in Figure 10 is not the same as the particle size distribution for the Davison 952 at 0 min before ultrasonic irradiation, as shown in Figure 7. The Davison 952 sample used for the ultrasonic fragmentation tests was sieved to obtain particle sizes between 45 and 103 μm. Sieving was done to see if the particle size distribution obtained from the Sedigraph 5100 analyzer was in agreement with the sample obtained after the sieving process (i.e., whether the analyzer was working properly). The as-received Davison 952 refers to the sample that was not sieved.

Discussion

Table 3 provides a qualitative summary of the attrition resistance as determined by ultrasonic fragmentation and the simulated F−T synthesis runs. These two methods rely on different mechanisms to cause attrition of the support agglomerates. Ultrasonic fragmentation relies on cavitation caused by collapse of bubbles in solution, while shear forces cause fragmentation during mixing in a STSR. The behavior of the supports with respect to their attrition resistance was generally similar, with some notable exceptions, despite the different approaches to fragmentation.

For example, the Vista B alumina and Davison 952 show similar extents of particle breakup (fracture) during both ultrasonic irradiation and STSR tests.

Table 3. Extent of Attrition after Ultrasonic Fragmentation and STSR Tests

		ultrasonic fragmentation		STSR tests	
support	morphology	fracture	erosion	fracture	erosion
		Alumina			
Vista HP 14	smooth, rounded	significant	small	moderate	significant
Vista HP 14-150	smooth, rounded	significant	small		
Vista B 965	irregular, fines visible	none	significant	none	small
		Silica			
Davison 644	irregular, fines visible	significant	none		
Davison 654		significant	significant		
Davison 948	smooth, rounded	small	none	moderate	small
Davison 952	irregular, fines visible	significant	significant	significant	significant

However, in the case of Vista HP 14 and Davison 948 supports, more erosion is seen after the STSR tests than during the corresponding ultrasonic irradiation tests. As expected, irregularly shaped, nonspherical Vista B alumina and Davison 952 particles had a greater extent of erosion in both ultrasonic fragmentation and STSR runs, in comparison to roughly spherical particles of HP 14 alumina and Davison 948 supports. However, a moderate extent of erosion was observed with Vista HP 14, and to a lesser extent with Davison 948 support, during the STSR tests. This shows that having nearly spherical, smooth shapes is not by itself sufficient to prevent erosion during F−T synthesis in slurry reactors.

One factor that needs to be considered when comparing results from ultrasonic irradiation and STSR tests is the extent of residual oil present on the support particles after the STSR tests. Residual oil may cause the fine particles generated during STSR runs to stick to the larger particles so that the Sedigraph 5100 analyzer may not be able to detect them. Residual oil could therefore interfere with the accuracy of the particle size analysis, which is performed in an aqueous solution. To avoid this artifact, we used a consistent washing procedure to remove the hydrocarbon oils from supports. Because some of the supports clearly show the generation of fine particles after long-term tests in the STSR, we feel confident that the observed results are indicative of the extent of attrition resistance of these particles.

Summary

We have investigated several commercially available aluminas and silicas for their potential use as supports for preparing attrition-resistant Fe F−T catalysts. After initial screening of these supports by the ultrasonic irradiation method, it was found that alumina supports were generally less attrition-resistant than the silica ones. Both fracture and erosion were observed with Vista HP 14-150 alumina. In contrast, there was no fracture of the particles of Vista B alumina, but erosion was observed both during ultrasonic fragmentation and during STSR tests. Among the silica supports, Davison 644 and 948 were more attrition-resistant than the alumina supports, particularly in terms of particle erosion. Davison 654 and 952 silicas showed considerable fracture and particle erosion. Results also showed that the STSR tests were more severe in terms of particle erosion compared to the ultrasonic irradiation approach, except for the Vista B alumina.

In future work, the attrition-resistant supports will be used to prepare Fe F−T catalysts. The prepared catalysts will then be tested in the STSR under actual F−T conditions to determine their catalytic performance (activity, selectivity, and stability with time). Slurry samples will be periodically withdrawn from the STSR in an inert atmosphere, and after separation of the catalyst from wax (slurry medium), particle size distribution measurements and catalyst characterization studies will be made. This will provide information on attrition properties of the working catalyst under reactive conditions.

Acknowledgment

We acknowledge financial support from the U.S. Department of Energy, National Energy Technology Laboratory, Grants DE-FG26-98FT40110 and DE-FG26-00NT40822.

Literature Cited

(1) Saxena, S. C. Bubble-Column Reactors and Fischer−Tropsch Synthesis. *Catal. Rev. Sci. Eng.* **1995**, *37*, 227.

(2) Bhatt, B. L.; Schaub, E. S.; Hedorn, E. C.; Herron, D. M.; Studer, D. W.; Brown, D. M. In *Proceedings of Liquefaction Contractors Review Conference*; Stiegel, G. J., Srivastava, R. D., Eds.; U.S. Department of Energy: Pittsburgh, PA, 1992; p 403.

(3) Jager, B.; Espinoza, R. Advances in Low-Temperature Fischer−Tropsch Synthesis. *Catal. Today* **1995**, *23*, 17.

(4) Thoma, S. G.; Ciftcioglu, M.; Smith, D. M. Determination of Agglomerate Strength Distributions. 1. Calibration via Ultrasonic Forces. *Powder Technol.* **1991**, *68*, 53.

(5) Thoma, S. G.; Ciftcioglu, M.; Smith, D. M. Determination of Agglomerate Strength Distributions. 3. Application to Titania Processing. *Powder Technol.* **1991**, *68*, 71.

(6) Pham, H. N.; Viergutz, A.; Gormley, R. J.; Datye, A. K. Improving the Attrition Resistance of Slurry Phase Heterogeneous Catalysts. *Powder Technol.* **2000**, *110*, 196.

(7) Pham, H. N.; Datye, A. K. Synthesis of Attrition-Resistant Heterogeneous Catalysts using Templated Mesoporous Silica. U.S. Patent 6,548,440, 2003.

(8) Pham, H. N.; Datye, A. K. The Synthesis of Attrition Resistant Slurry Phase Iron Fischer−Tropsch Catalysts. *Catal. Today* **2000**, *58*, 233.

(9) Srinivasan, R.; Xu, L.; Spicer, R. L.; Tungate, F. L.; Davis, B. H. Fischer−Tropsch Catalysts. Attrition of Carbided Iron Catalyst in the Slurry Phase. *Fuel Sci. Technol. Int.* **1996**, *14*, 1337.

(10) Jothimurugesan, K.; Goodwin, J. G., Jr.; Gangwal, S. K.; Spivey, J. J. Development of Fe Fischer−Tropsch Catalysts for Slurry Bubble Column Reactors. *Catal. Today* **2000**, *58*, 335.

(11) Zhao, R.; Goodwin, J. G., Jr.; Jothimurugesan, K.; Gangwal, S. K.; Spivey, J. J. Spray Dried Iron Fischer−Tropsch Catalysts. 1. Effect of Structure on the Attrition Resistance of the Catalysts in the Calcined State. *Ind. Eng. Chem. Res.* **2001**, *40*, 1065.

(12) O'Brien, R. J.; Xu, L.; Bao, S.; Raje, A.; Davis, B. H. Activity, Selectivity and Attrition Characteristics of Supported Iron Fischer−Tropsch Catalysts. *Appl. Catal. A* **2000**, *196*, 173.

(13) Bukur, D. B.; Sivaraj, C. Supported Iron Catalysts for Slurry Phase Fischer−Tropsch Synthesis. *Appl. Catal. A* **2002**, *231*, 201.

(14) Bukur, D. B.; Lang, X.; Rossin, J. A.; Zimmerman, W. H.; Rosynek, M. P.; Yeh, E. B.; Li, C. Activation Studies with a Promoted Precipitated Iron Fischer−Tropsch Catalyst. *Ind. Eng. Chem. Res.* **1989**, *28*, 1130.

(15) Bukur, D. B.; Nowicki, L.; Patel, S. A. Activation Studies with an Iron Fischer−Tropsch Catalyst in Fixed Bed and Stirred Tank Slurry Reactors. *Can. J. Chem. Eng.* **1996**, *74*, 399.

(16) Bukur, D. B.; Nowicki, L.; Lang, X. Fischer−Tropsch Synthesis in a Stirred-Tank Slurry Reactor. *Chem. Eng. Sci.* **1994**, *49*, 4615.

(17) Pham, H. N.; Reardon, J.; Datye, A. K. Measuring the Strength of Slurry Phase Heterogeneous Catalysts. *Powder Technol.* **1999**, *103*, 95.

(18) Zhao, R.; Goodwin, J. G., Jr.; Oukaci, R. Attrition Assessment for Slurry Bubble Column Reactor Catalysts. *Appl. Catal. A* **1999**, *189*, 99.

Received for review November 4, 2002
Revised manuscript received May 15, 2003
Accepted May 16, 2003

IE020875H